On Secrecy Performance of MISO SWIPT Systems with TAS and Imperfect CSI

Gaofeng Pan, $Member, IEEE$, Hongjiang Lei, Yansha Deng, Lisheng Fan, Jing Yang, Yunfei Chen, $SeniorMember, IEEE$ and Zhiguo Ding, $SeniorMember, IEEE$

***Abstract*—In this work, a multiple-input single-output (MISO) simultaneous wireless information and power transfer (SWIPT) system including one base station (BS) equipped with multiple antennas, one desired single-antenna information receiver (IR) and N ($N > 1$) single-antenna energy-harvesting receivers (ERs) is considered. Assuming that the information signal to the desired IR may be eavesdropped by ERs if ERs are malicious, we investigate the secrecy performance of the target MISO SWIPT system when imperfect channel state information (CSI) is available and adopted for transmit antenna selection at the BS. Considering that each eavesdropping link experiences independent but not necessarily identically distributed Rayleigh fading, the closed-form expressions for the exact and the asymptotic secrecy outage probability, and the average secrecy capacity are derived and verified by simulations. Furthermore, the optimal power splitting factor is derived for each ER to realize the tradeoff between the energy harvesting and the information eavesdropping. Our results reveal the impact of the imperfect CSI on the secrecy performance of MISO SWIPT systems in the presence of multiple wiretap channels.**

***Index Terms*—Channel state information, multiple-input single-output, secrecy capacity, secrecy outage probability, simultaneous wireless information and power transfer.**

I. Introduction

As a safe, green and convenient energy harvesting (EH) solution to energy-constrained communication systems, simultaneous wireless information and power transfer (SWIPT) has gained a great deal of attention, which adopts the same emitted electromagnetic wave to transport both energy that can be harvested at the receiver, and information that can be decoded by the receiver [1]-[2].

G. Pan is with the School of Electronic and Information Engineering, Southwest University, Chongqing, 400715, China. He is also with School of Computing and Communications, Lancaster University, Lancaster, LA1 4YW, U.K. e-mail: pan.156@osu.edu.

H. Lei is with the Chongqing Key Lab of Mobile Communications Technology, Chongqing University of Posts and Telecommunications, Chongqing 400065, China.

Y. Deng is with Centre for Telecommunications, King's College London, WC2R 2LS, UK.

L. Fan is with the Department of Electronic Engineering, Shantou University, Shantou 515063, China,

J. Yang is with School of Information Engineering, Yangzhou University, Yang Zhou, 225009, China.

Y. Chen is with the School of Engineering, University of Warwick, Coventry, CV4 7AL, U.K.

Z. Ding is with School of Computing and Communications, Lancaster University, Lancaster, LA1 4YW, U.K.

This research was supported in part by the National Science Foundation under Grants 61401372 and 61531016, Research Fund for the Doctoral Program of Higher Education of China under Grant 20130182120017, Natural Science Foundation of CQ CSTC under Grant cstc2013jcyjA40040, the Fundamental Research Funds for the Central Universities under Grant XDJK2015B023 and XDJK2016A011.

Initial research works in the field of SWIPT focused on single-input-single-output (SISO) systems [1]-[3]. Motivated by benefits of multi-antenna techniques, multiple-input single-output (MISO) and multiple-input-multiple-output (MIMO) SWIPT systems have drawn considerable attention in [4]-[11] and [12]-[19], respectively. However, these aforementioned works were carried out assuming that the perfect channel state information (CSI) was available. In practice, it is difficult to obtain perfect CSI because of channel estimation and quantization errors [20]-[21]. Specially, in fact, the energy receivers (ERs) are not continuously interacting with the transmitter and the corresponding CSI at the transmitter may be outdated even if the channel is only slowly time varying [22].

Recently, some works have studied MISO SWIPT systems considering imperfect CSI [22]-[29]. In a downlink MSIO SWIPT system, a resource allocation algorithm was proposed in [22] to minimize the total transmitting power in the presence of passive eavesdroppers and potential eavesdroppers (idle legitimate receivers) for the case when the legitimate receivers are able to harvest energy from radio frequency (RF) signals. In [23], a cooperative jamming aided robust secure transmission scheme for SWIPT in MISO channels has been proposed where it is assumed that the source and the cooperative jammer know imperfect CSI. In a power splitting (PS)-based MISO interference channel for SWIPT, the authors of [24] minimized the total transmission power by joint beamforming and PS under both the signal-to-interference-plus-noise ratio (SINR) and EH constraints in the presence of local CSI. In [25], the joint multicast transmit beamforming and receive PS problem was investigated for MISO SWIPT systems to minimize the transmit power of the transmitter subject to signal-to-noise ratio (SNR) and EH constraints at each receiver, while considering both scenarios of perfect and imperfect CSI at the transmitter. In [26], a downlink MISO SWIPT system was considered with imperfect CSI at the transmitter and two robust joint beamforming and PS designs were developed to minimize the transmission power under both the SINR and EH constraints per user. Considering the imperfect CSI of idle secondary receivers and primary receivers, the authors of [29] studied the resource allocation algorithm design for cognitive radio secondary networks with simultaneous wireless power transfer and secure communication based on a multiobjective optimization framework.

Meanwhile, some other works have been presented to study MIMO SWIPT systems with imperfect CSI in [30]-[35]. [30] investigated MIMO communications under EH constraints and studied the beamforming designs with partial CSI. The

authors of [31] proposed an optimal and the low complexity suboptimal energy efficient power allocation algorithms for MIMO SWIPT systems with covariance CSI feedback. In [32], the authors studied the robust beamforming problem for the multi-antenna SWIPT systems to maximize the worst-case harvested energy for the ER, while guaranteeing that the rate for the information receiver (IR) is above a threshold, under the assumption of imperfect CSI at the transmitter. In a MIMO SWIPT system, the authors of [33] analyzed and derived closed-form representations of the ergodic downlink rate, and both the energy shortage and data outage probability were derived for the three cases of CSI at the transmitter: no CSI, and imperfect CSI in case of time-division duplexing and frequency-division duplexing communications. In a MIMO SWIPT system, the authors of [27] investigated the robust secure transmission scheme to maximize the worst-case secrecy rate under transmitting power constraint and EH constraint while considering channel uncertainties. A robust artificial noise-aided secure transmission design was studied in [28] for MIMO SWIPT systems, where the channel uncertainties are modeled by worst-case model. In a MISO SWIPT system, the harvested energy by the ERs was maximized while maintaining the SINR threshold at the IR and keeping the message secure from possible eavesdropping by the ERs by suppressing their SINRs in both scenarios of perfect and imperfect CSI at the transmitter [34]. [35] addressed the ergodic secrecy rate maximization problem subject to a harvested energy constraint in the MIMO SWIPT wiretap channel under the assumption of only statistical CSI at the transmitter.

In SWIPT systems, an energy signal is transmitted along with the information signal to expedite EH at the ERs. In practice, the transmitter could increase the transmitting power of the information carrying signal to facilitate EH at the ERs. However, this may also lead to an increased susceptibility to eavesdropping due to a higher potential for information leakage when ERs are malicious. Therefore, a new quality of service concern on communication security arises in SWIPT systems, which is very important to tackle. In fact, security is also a fundamental problem in common wireless systems due to the broadcast nature of the wireless medium [36]. The most recent advance in physical (PHY) layer security is to exploit the PHY characteristics of the wireless fading channels for perfect secrecy of communication, especially there are some works have been presented to studied the PHY secrecy of the traditional wireless systems while considering imperfect CSI [37]-[43]. However, none of them is related to SWIPT systems.

Clearly, these aforementioned investigations [3]-[35] were mainly presented on power control, transmission strategy and resource scheduling to optimize the performance of SWIPT systems. Some of them, such as [3], [5], [8]-[11], [16]-[19], [22]-[23], [27]-[29], [34]-[35], studied the secrecy transmission in SWIPT while considering perfect/imperfect CSI. Making use of artificial noise method, the authors of [44] designed a joint information and energy transmit beamforming scheme to maximize the secrecy rate of the IR in a secret MISO SWIPT system. However, it is clear that the existing literature on the PHY security of SWIPT systems is limited to transmission scheme design or resource allocation. In [45], the secrecy performance (secrecy outage and secrecy capacity) has been studied for single-input multiple-output SWIPT systems. To the best of authors knowledge, there have been no previous results reported on the secrecy performance analysis for SWIPT systems in the presence of imperfect CSI.

In this paper, a MISO SWIPT system consisting of one BS equipped with multiple antennas, one desired IR and N ($N > 1$) ERs is considered. In particular, we focus on the physical layer security performance including secrecy outage probability (SOP) and the average secrecy capacity (ASC) in the presence of eavesdroppers (ERs). Main contributions of this work are as follows:

(1) We derive the closed-form analytical expression for the exact and the asymptotic secrecy outage probability while considering imperfect CSI and each eavesdropping link experiences independent but not necessarily identical Rayleigh fading.

(2) The closed-form analytical expression for the ASC has also been derived for the case that all eavesdropping links experience independent but not necessarily identical Rayleigh fading in the presence of imperfect CSI.

(3) The optimal PS factor is derived for each ER to realize the tradeoff between the EH and the information eavesdropping.

Making use of our proposed analysis models, during the design or optimization of the targeted MISO SWIPT system, the secrecy performance of the targeted system can be precisely evaluated for different system settings, such as the number of the antennas at BS and IR, and the number of ERs. Especially, our derived models can be applied to the scenarios of i.n.d. Nakagami-m fading channels, which are more common in practical applications.

This paper is structured as follows. In Section II, the system model in the presence of imperfect CSI is presented. The analysis on secrecy outage performance is presented in Section III. In Section IV, the ASC of the considered system is analyzed. The method on deriving the optimal PS factor is presented in Section V. The proposed analytical models are verified by Monte-Carlo simulations in Section VI. Finally, the paper is concluded in Section VI.

II. System model

In this paper, we consider a multi-user MISO downlink SWIPT system consisting of one BS equipped with N_T ($N_T > 1$) antennas, one desired IR and N ($N > 1$) ERs, denoted by ER_1, $\cdots$, ER_N, respectively, over a given frequency band, which have a single antenna, as shown by Fig. 1 in [45]. It is assumed that all links between BS and IR experience independent and identically Rayleigh fading with same and all links between BS and ERs experience independent but not necessarily identical Rayleigh fading.

We assume that IR feedbacks the CSI to BS and that the CSI of the links between ERs and BS is also available at BS (this is reasonable as ERs are also the legal users in the system). However, ERs may play as passive eavesdroppers, as BS can adapt transmission rate according to both CSI of the BS-IR channel and BS-ER channels to achieve perfect

secure transmission. IR only needs to compare the received signals over the links between each transmitting antenna and itself, and then feedback the corresponding antenna index to BS. The feedback information can be represented by a binary vector with $\log N_{\mathrm{T}}$ bits.

The CSI feedback from IR is delayed and BS encodes the message to Bob by making use of IR's outdated CSI to select a single transmit antenna which yields the maximum instantaneous SNR[1]. Then, the largest channel gain of the links between the selected antenna at BS and IR at the time of selection can be expressed as

$$\tilde{g} = \max_{k\in\{1,\cdots,N_T\}} \{\tilde{g}_k\}, \tag{1}$$

where $\tilde{g}_k$ is the delayed channel coefficient between BS's kth antenna and IR, which is different from the actual channel coefficient between BS's kth antenna and IR denoted as g_k.

After the antenna selection, BS delivers information to IR and transfers energy to all ERs simultaneously. All EH receivers are supposed to harvest energy from the RF. However, the signals intended for the desired IR may be overheard by all ERs since all EH receivers are in the coverage range. If ERs are malicious, they may eavesdrop the information signal of the desired IR. Hence, all ERs are potential eavesdroppers which should be considered. In this work, we assume that all ERs work independently and no information exchange exists among these ERs.

In this work, it is also assumed that each ER adopts PS method to perform information decoding and EH from the received signal [12]. Specifically, as shown in Fig. 2 in [12] and [45], the received signal at each EH is split to the information decoding (ID) and the EH by a power splitter, which divides an ρ_i $(0 \le \rho_i \le 1)$ portion of the signal power to the ID, and the remaining $1-\rho_i$ portion of power to the EH.

Then, the received signal in the downlink is given by

$$y_{\mathrm{IR}} = \sqrt{P_t L_c {d_{\mathrm{B,I}}}^{-\kappa}} g s + n_{\mathrm{IR}} \tag{2-a}$$

$$y_{\mathrm{EH}i} = \sqrt{\rho_i}\left(\sqrt{P_t L_c {d_{\mathrm{B,E}_i}}^{-\kappa}} h_i s + n_{\mathrm{EH}i}\right) + z_i, \tag{2-b}$$

respectively, where P_t is the transmitting power at BS, $L_c = G_T G_R \left(\frac{c}{4\pi f}\right)^2$ is the path loss constant[2] (where G_T and G_R are the antenna gains of the transmitter and the receiver, respectively, c is the speed of light, and f is the carrier frequency), $d_{\mathrm{B,I}}$ is the distance between BS and IR, $d_{\mathrm{B,E}_i}$ is the distance between BS and ith $(i \in \{1,\cdots,N\})$ ER, κ, which is typically between 2.7 and 3.5, is the path-loss exponent (when $\kappa = 0$, it means ignoring the effect of path-loss), g is the channel gain of the link between the selected transmit antenna at BS and IR, s denotes the transmitted symbols from BS, h_i is the link channel gain between the selected transmit antenna at BS and the ith EH receiver, n_{IR} and $n_{\mathrm{EH}i}$ denote the independent complex Gaussian noise at the desired IR and the ith EH receiver, respectively. In this work, to simplify the analysis, we assume that n_{IR} and $n_{\mathrm{EH}i}$ have zero means and the same variances, N_0, z_i is the signal processing noise by the ID at the ith EH, which can also be modeled as additional white Gaussian noise with means zero and variances σ_i^2. The correlation relationship between $\tilde{g}_k$ and g_k can be modeled as

$$\tilde{g}_k = \sqrt{\eta} g_k + \sqrt{1-\eta}\omega_k, \tag{3}$$

where ω_k represents a complex Gaussian variable with zero mean and variance $\sigma^2_{\mathrm{IR}_k}$, where $\sigma^2_{\mathrm{IR}_k}$ is the variance of g_k, η is given by [20]-[21]

$$\eta = \left[J_0\left(2\pi f_d \tau\right)\right]^2, \tag{4}$$

where $J_0(\cdot)$ denotes the 0th order Bessel function of first kind as defined by Eq. (8.402) in [48] and f_d indicates the maximum Doppler frequency.

The SNR of the signal at IR and the ID at $\mathrm{EH_i}$ can be written from (2) as

$$\gamma_g = \frac{P_t L_c |g|^2}{N_0 {d_{\mathrm{B,I}}}^{\kappa}} \tag{5-a}$$

$$\gamma_{\mathrm{EH}i} = \frac{\rho_i P_t L_c |h_i|^2}{{d_{\mathrm{B,E}_i}}^{\kappa}\left(\rho_i N_0 + \sigma_i^2\right)}. \tag{5-b}$$

Therefore, the instantaneous secrecy capacity can be presented as

$$C_s\left(\gamma_g, \gamma_{\max}\right) = \left[\log_2\left(1+\gamma_g\right) - \log_2\left(1+\gamma_{\max}\right)\right]^+, \tag{6}$$

where $[x]^+$ denotes $\max\{x, 0\}$, $\gamma_{\max} = \max\limits_{i\in\{1,\cdots,N\}} \{\gamma_{\mathrm{EH}i}\}$.

The probability density function (PDF) of $|\tilde{g}_k|^2$ and $|h_i|^2$ can be given as

$$f_{|\tilde{g}_k|^2}(x) = \frac{1}{g_{\mathrm{A}}} \exp\left(-\frac{x}{g_{\mathrm{A}}}\right) \tag{7}$$

$$f_{|h_i|^2}(x) = \frac{1}{h_{\mathrm{A}i}} \exp\left(-\frac{x}{h_{\mathrm{A}i}}\right), \tag{8}$$

respectively, where g_{A} and $h_{\mathrm{A}i}$ are the expectation of channel power gain $|\tilde{g}_k|^2$ and $|h_i|^2$, respectively.

Then, we can obtain $\gamma_{\tilde{g}_k} = \frac{P_t L_c}{{d_{\mathrm{B,I}}}^{\kappa} N_0}|\tilde{g}_k|^2 \sim \mathrm{Exp}(\lambda_A)$ and $\gamma_{\mathrm{EH}i} \sim \mathrm{Exp}(\lambda_{\mathrm{EH}i})$, where $\lambda_A = \frac{{d_{\mathrm{B,I}}}^{\kappa} N_0}{g_{\mathrm{A}} P_t L_c}$ and $\lambda_{\mathrm{EH}i} = \frac{{d_{\mathrm{B,E}_i}}^{\kappa}\left(\rho_i N_0 + \sigma_i^2\right)}{h_{\mathrm{A}i}\rho_i P_t L_c}$.

[1]SWIPT technology is mostly used in the systems with low-energy-budget and low-hardware-complexity terminals, e.g., wireless sensor networks. So the transmit diversity technologies (like maximum ratio transmission), which require the terminals to calculate and feed back the CSI of all links, are impractical for typical SWIPT systems. Further, more resource would be required at the terminal to process the multiple copies of the signals from each antenna during the date delivery, leading to increased hardware complexity and cost.

TAS scheme is a good tradeoff between the diversity gain and the implementation cost, as the terminal only needs to compare and feed back the corresponding antenna index. As suggested by [46], the terminal can perfectly distinguish the multiple copies of the pilot signals from each transmit antenna using a time division multiple access based TAS implementation scheme. Also, TAS has the advantage of using one antenna equipped with one RF chain compared to other techniques that require multiple RF chains corresponding to the number of antennas. Therefore, in this work TAS scheme is considered at BS.

[2]In this work, we consider the classic flat earth model as the path loss model [47].

Further, it is easy to obtain the PDF of $\gamma_{\max}$ as

$$f_{\gamma_{\max}}(x)=\sum_{i=1}^{N}\lambda_{\mathrm{EH}i}\exp\left(-\lambda_{\mathrm{EH}i}x\right)\prod_{\substack{j=1\\ j\neq i}}^{N}\left[1-\exp\left(-\lambda_{\mathrm{EH}j}x\right)\right]. \tag{9}$$

The PDF of $\gamma_{\tilde{g}}=\frac{P_tL_c|\tilde{g}|^2}{N_0d_{\mathrm{B,I}}{}^{\kappa}}$ can be written as

$$f_{\gamma_{\tilde{g}}}(x)=N_T\left[F_{\gamma_{\tilde{g}_k}}(x)\right]^{N_T-1}f_{\gamma_{\tilde{g}_k}}(x), \tag{10}$$

where $F_{\gamma_{\tilde{g}_k}}(x)$ is the cumulative distribution function of $\gamma_{\tilde{g}_k}$.

As all links between each antenna at the BS and IR experience independent and identically Rayleigh fading, the PDF of γ_g can be obtained as

$$f_{\gamma_g}(x)=\int_0^{\infty}f_{\gamma_g|\gamma_{\tilde{g}}}(x|\,y)f_{\gamma_{\tilde{g}}}(y)\,dy, \tag{11}$$

where $f_{\tilde{\gamma}_g|\gamma_g}(x|\,y)$ is the joint PDF of γ_g and $\gamma_{\tilde{g}}$ (for a correlation coefficient η) is given by [49]

$$f_{\gamma_g|\gamma_{\tilde{g}}}(x|\,y)=\frac{\lambda_A}{1-\eta}\exp\left(-\lambda_A\frac{x+\eta y}{1-\eta}\right)\cdot I_0\left(\frac{2\lambda_A\sqrt{\eta xy}}{1-\eta}\right), \tag{12}$$

where $I_0(\cdot)$ is the 0th order modified Bessel function of first kind as defined by Eq. (8.406) in [48].

Then, substituting (10) and (12) into (11), the PDF of γ_g can be

$$\begin{aligned}f_{\gamma_g}(x)=&\int_0^{\infty}\frac{\lambda_A}{1-\eta}\exp\left(-\lambda_A\frac{x+\eta y}{1-\eta}\right)\cdot I_0\left(\frac{2\lambda_A\sqrt{\eta xy}}{1-\eta}\right)\\&\cdot N_T\left[F_{\gamma_{\tilde{g}_k}}(y)\right]^{N_T-1}f_{\gamma_{\tilde{g}_k}}(y)\,dy\\=&\frac{N_T(\lambda_A)^2}{1-\eta}\exp\left(-\frac{\lambda_A}{1-\eta}x\right)\int_0^{\infty}\exp\left(-\frac{\lambda_A}{1-\eta}y\right)\\&\cdot\left[1-\exp\left(-\lambda_Ay\right)\right]^{N_T-1}\cdot I_0\left(\frac{2\lambda_A\sqrt{\eta xy}}{1-\eta}\right)dy\\=&\frac{N_T(\lambda_A)^2}{1-\eta}\exp\left(-\frac{\lambda_A}{1-\eta}x\right)\sum_{i=0}^{N_T-1}\binom{N_T-1}{i}(-1)^i\\&\cdot\int_0^{\infty}\exp\left(-\lambda_A\left(\frac{1}{1-\eta}+i\right)y\right)\cdot I_0\left(\frac{2\lambda_A\sqrt{\eta xy}}{1-\eta}\right)dy.\end{aligned} \tag{13}$$

Let $z=\sqrt{y}$, $dy=2zdz$. Then, by using Eq. (2.15.5.4) in [50], the integral in last equation can be written as

$$\begin{aligned}&\int_0^{\infty}\exp\left(-\lambda_A\left(\frac{1}{1-\eta}+i\right)y\right)\cdot I_0\left(\frac{2\lambda_A\sqrt{\eta xy}}{1-\eta}\right)dy=\\&2\int_0^{\infty}z\exp\left(-\lambda_A\left(\frac{1}{1-\eta}+i\right)z^2\right)\cdot I_0\left(\frac{2\lambda_A\sqrt{\eta x}}{1-\eta}z\right)dz\\&=\lambda_A{}^{-1}\left(\frac{1}{1-\eta}+i\right)^{-1}\exp\left(\frac{\eta\left(\frac{\lambda_A}{1-\eta}\right)^2x}{\lambda_A\left(\frac{1}{1-\eta}+i\right)}\right).\end{aligned} \tag{14}$$

Substituting (14) into (13), we obtain

$$\begin{aligned}f_{\gamma_g}(x)=&N_T\sum_{i=0}^{N_T-1}\binom{N_T-1}{i}\frac{(-1)^i\lambda_A}{1+(1-\eta)i}\\&\cdot\exp\left(-\frac{\lambda_A(i+1)}{1+(1-\eta)i}x\right)\\=&N_T\sum_{i=0}^{N_T-1}\binom{N_T-1}{i}(-1)^iA_i\exp(-B_ix),\end{aligned} \tag{15}$$

where $A_i=\frac{\lambda_A}{1+(1-\eta)i}$ and $B_i=A_i(i+1)$.

III. Secrecy outage analysis

In this paper, SOP is defined as the probability that instantaneous secrecy capacity is below a threshold secrecy rate, C_{th} ($C_{th}\geq 0$). Then, SOP can be written as

$$\begin{aligned}SOP(C_{th})=&\Pr\{C_s\leq C_{th}\}\\=&\Pr\left\{\frac{1+\gamma_g}{1+\gamma_{\max}}\leq 2^{C_{th}}\right\}\\=&\Pr\left\{\gamma_g\leq\alpha\left(1+\gamma_{\max}\right)-1\right\},\end{aligned} \tag{16}$$

where $\alpha=2^{C_{th}}$.

For simplification, let $\lambda_i=\lambda_{\mathrm{EH}i}$ in the rest of the paper. Then, we can rewrite (8) as

$$f_{\gamma_{\max}}(x)=\sum_{i=1}^{N}\lambda_i\exp\left(-\lambda_ix\right)\prod_{\substack{j=1\\ j\neq i}}^{N}\left[1-\exp\left(-\lambda_jx\right)\right]. \tag{17}$$

Further, we can obtain

$$\begin{aligned}\prod_{\substack{j=1\\ j\neq i}}^{N}\left[1-\exp\left(-\lambda_jx\right)\right]=&\sum_{p=0}^{N-1}(-1)^p\cdot\sum_{m=1}^{\binom{|\Omega_{N,i}|}{p}}\\&\cdot\exp\left(-\boldsymbol{\lambda}_{p,m}^T\mathbf{I}_px\right)\\=&\sum\nolimits_p\sum\nolimits_m\exp\left(-\boldsymbol{\lambda}_{p,m}^T\mathbf{I}_px\right),\end{aligned} \tag{18}$$

where $\Omega_{N,i}=\{\lambda_1,\lambda_2,\cdots,\lambda_N\}-\{\lambda_i\}$, $|\Omega_{N,i}|$ denotes the number of the elements in $\Omega_{N,i}$, $(\cdot)^T$ denotes the transpose operator, $\boldsymbol{\lambda}_{p,m}$ is the vector of $\Omega_{N,i,m,p}\cup\{0\}$, $\Omega_{N,i,m,p}$ is the mth ($1\leq m\leq\binom{|\Omega_{N,i}|}{p}$) subset with p elements of $\Omega_{N,i}$, $\mathbf{I}_p$ is the unit vector with $(1+p)$ elements. In the following, we use $\sum_p\sum_m$ instead of $\sum_{p=0}^{N-1}(-1)^p\cdot\sum_{m=1}^{\binom{|\Omega_{N,i}|}{p}}$ for simplification.

Then, making use of (18), (17) can be written as

$$\begin{aligned}f_{\gamma_{\max}}(x)=&\sum_{i=1}^{N}\lambda_i\exp\left(-\lambda_ix\right)\sum\nolimits_p\sum\nolimits_m\exp\left(-\boldsymbol{\lambda}_{p,m}^T\mathbf{I}_px\right)\\=&\sum_{i=1}^{N}\lambda_i\sum\nolimits_p\sum\nolimits_m\exp\left(-\Theta_ix\right),\end{aligned} \tag{19}$$

where $\Theta_i = \boldsymbol{\lambda}_{p,m}^T \mathbf{I}_p + \lambda_i$.

Therefore, we can obtain

$$\begin{aligned} SOP\left(C_{th}\right) &= \int_0^{\infty} \int_0^{\alpha(1+y)-1} f_{\gamma_g}\left(x\right) f_{\gamma_{\max}}\left(y\right) dxdy \\ &= N_T \sum_{i=0}^{N_T-1} \binom{N_T-1}{i} \left(-1\right)^i A_i \int_0^{\infty} f_{\gamma_{\max}}\left(y\right) \\ &\quad \cdot \int_0^{\alpha(1+y)-1} \exp\left(-B_i x\right) dxdy \\ &= N_T \sum_{i=0}^{N_T-1} \binom{N_T-1}{i} \frac{\left(-1\right)^i A_i}{B_i} \\ &\quad \cdot \int_0^{\infty} f_{\gamma_{\max}}\left(y\right) \left[1 - \exp\left(-B_i \alpha y - B_i \alpha + B_i\right)\right] dy \\ &= I_1 + I_2, \end{aligned} \tag{20}$$

where

$$I_1 = N_T \sum_{i=0}^{N_T-1} \binom{N_T-1}{i} \frac{\left(-1\right)^i A_i}{B_i} \int_0^{\infty} f_{\gamma_{\max}}\left(y\right) dy$$

and

$$I_2 = -N_T \sum_{i=0}^{N_T-1} \binom{N_T-1}{i} \frac{\left(-1\right)^i A_i}{B_i} \exp\left(-B_i \alpha + B_i\right) \cdot \int_0^{\infty} f_{\gamma_{\max}}\left(y\right) \exp\left(-B_i \alpha y\right) dy.$$

Making use of (19), we can rewrite I_1 and I_2 as

$$\begin{aligned} I_1 &= N_T \sum_{i=0}^{N_T-1} \binom{N_T-1}{i} \frac{\left(-1\right)^i A_i}{B_i} \sum_{j=1}^{N} \lambda_j \sum\nolimits_p \sum\nolimits_m \\ &\quad \cdot \int_0^{\infty} \exp\left(-\Theta_j y\right) dy \\ &= N_T \sum_{i=0}^{N_T-1} \binom{N_T-1}{i} \frac{\left(-1\right)^i A_i}{B_i} \sum_{j=1}^{N} \lambda_j \sum\nolimits_p \sum\nolimits_m \frac{1}{\Theta_j}, \end{aligned} \tag{21}$$

$$\begin{aligned} I_2 &= -N_T \sum_{i=0}^{N_T-1} \binom{N_T-1}{i} \frac{\left(-1\right)^i A_i}{B_i} \exp\left(-B_i \alpha + B_i\right) \\ &\quad \cdot \sum_{j=1}^{N} \lambda_j \sum\nolimits_p \sum\nolimits_m \int_0^{\infty} \exp\left(-\left(\Theta_j + B_i \alpha\right) y\right) dy \\ &= -N_T \sum_{i=0}^{N_T-1} \binom{N_T-1}{i} \frac{\left(-1\right)^i A_i}{B_i} \exp\left(-B_i \alpha + B_i\right) \\ &\quad \cdot \sum_{j=1}^{N} \lambda_j \sum\nolimits_p \sum\nolimits_m \frac{1}{\Theta_j + B_i \alpha}, \end{aligned} \tag{22}$$

respectively.

Then, SOP can be obtained by substituting (21) and (22) into (20).

In the following, we will derive the asymptotic SOP while $\bar{\gamma}_A = \frac{P_t g_{\mathrm{A}} L_c}{N_0 {d_{\mathrm{B,I}}}^{\eta}} \to \infty$ (namely, $\bar{\gamma}_A = {\lambda_A}^{-1} \to \infty$). Then, we can rewrite (15) as

$$f_{\gamma_g}\left(x\right) = \frac{N_T}{\bar{\gamma}_A} \sum_{i=0}^{N_T-1} \binom{N_T-1}{i} \frac{\left(-1\right)^i}{A_i'} \exp\left(-\frac{B_i'}{\bar{\gamma}_A} x\right), \tag{23}$$

where $A_i' = 1 + (1-\eta)i$ and $B_i' = \frac{i+1}{1+(1-\eta)i}$.

Using the Taylor series expansion of the exponential function in (23) given by $\exp\left(-\frac{B_i'}{\bar{\gamma}_A} x\right) = \sum_{l=0}^{\infty} \frac{\left(-\frac{B_i'}{\bar{\gamma}_A} x\right)^l}{l!}$ and only keeping the first two terms while neglecting the higher order terms, we can rewrite SOP in (20) as

$$\begin{aligned} SOP\left(C_{th}\right) &\approx \int_0^{\infty} \int_0^{\alpha(1+y)-1} f_{\gamma_g}\left(x\right) f_{\gamma_{\max}}\left(y\right) dxdy \\ &= \frac{N_T}{\bar{\gamma}_A} \sum_{i=0}^{N_T-1} \binom{N_T-1}{i} \frac{\left(-1\right)^i}{\mathrm{A}_i'} \int_0^{\infty} f_{\gamma_{\max}}\left(y\right) \\ &\quad \cdot \int_0^{\alpha(1+y)-1} \left(1 - \frac{B_i'}{\bar{\gamma}_A} x\right) dxdy \\ &= \frac{N_T}{\bar{\gamma}_A} \sum_{i=0}^{N_T-1} \binom{N_T-1}{i} \frac{\left(-1\right)^i}{\mathrm{A}_i'} \\ &\quad \cdot \int_0^{\infty} f_{\gamma_{\max}}\left(y\right) \left(C_1 y^2 + C_2 y + C_3\right) dy \\ &= D_1 + D_2 + D_3, \end{aligned} \tag{24}$$

where $C_1 = -\frac{B_i'}{2\bar{\gamma}_A}\alpha^2$, $C_2 = \alpha\left(1 + \frac{B_i'}{\bar{\gamma}_A} - \frac{B_i'}{\bar{\gamma}_A}\alpha\right)$, $C_3 = \alpha - 1 - \left(1 - 2\alpha + \alpha^2\right)\frac{B_i'}{2\bar{\gamma}_A}$,

$$D_1 = \frac{N_T}{\bar{\gamma}_A} \sum_{i=0}^{N_T-1} \binom{N_T-1}{i} \frac{\left(-1\right)^i C_1}{\mathrm{A}_i'} \int_0^{\infty} f_{\gamma_{\max}}\left(y\right) y^2 dy,$$

$$D_2 = \frac{N_T}{\bar{\gamma}_A} \sum_{i=0}^{N_T-1} \binom{N_T-1}{i} \frac{\left(-1\right)^i C_2}{\mathrm{A}_i'} \int_0^{\infty} f_{\gamma_{\max}}\left(y\right) y dy,$$

and

$$D_3 = \frac{N_T}{\bar{\gamma}_A} \sum_{i=0}^{N_T-1} \binom{N_T-1}{i} \frac{\left(-1\right)^i C_3}{\mathrm{A}_i'} \int_0^{\infty} f_{\gamma_{\max}}\left(y\right) dy.$$

Making use of (19) and Eq. (3.351.3) in [48], we can rewrite D_1, D_2 and D_3 as

$$\begin{aligned} D_1 &= \frac{N_T}{\bar{\gamma}_A} \sum_{i=0}^{N_T-1} \binom{N_T-1}{i} \frac{\left(-1\right)^i C_1}{\mathrm{A}_i'} \sum_{j=1}^{N} \lambda_j \sum\nolimits_p \sum\nolimits_m \\ &\quad \cdot \int_0^{\infty} y^2 \exp\left(-\Theta_j y\right) dy \end{aligned}$$

$$= \frac{2N_T}{\bar{\gamma}_A} \sum_{i=0}^{N_T-1} \left(\begin{array}{c} N_T-1 \\ i \end{array} \right) \frac{(-1)^i \mathrm{E}_1}{\mathrm{A}_i'} \sum_{j=1}^{N} \lambda_j \sum\nolimits_p \sum\nolimits_m \Theta_j^{-3} \quad (25-a)$$

$$D_2 = \frac{N_T}{\bar{\gamma}_A} \sum_{i=0}^{N_T-1} \left(\begin{array}{c} N_T-1 \\ i \end{array} \right) \frac{(-1)^i C_2}{\mathrm{A}_i'} \sum_{j=1}^{N} \lambda_j \sum\nolimits_p \sum\nolimits_m \cdot \int_0^{\infty} y \exp\left(-\Theta_j y\right) dy$$

$$= \frac{N_T}{\bar{\gamma}_A} \sum_{i=0}^{N_T-1} \left(\begin{array}{c} N_T-1 \\ i \end{array} \right) \frac{(-1)^i C_2}{\mathrm{A}_i'} \sum_{j=1}^{N} \lambda_j \sum\nolimits_p \sum\nolimits_m \Theta_j^{-2} \quad (25-b)$$

$$D_3 = \frac{N_T}{\bar{\gamma}_A} \sum_{i=0}^{N_T-1} \left(\begin{array}{c} N_T-1 \\ i \end{array} \right) \frac{(-1)^i C_3}{\mathrm{A}_i'} \sum_{j=1}^{N} \lambda_j \sum\nolimits_p \sum\nolimits_m \cdot \int_0^{\infty} \exp\left(-\Theta_j y\right) dy$$

$$= \frac{N_T}{\bar{\gamma}_A} \sum_{i=0}^{N_T-1} \left(\begin{array}{c} N_T-1 \\ i \end{array} \right) \frac{(-1)^i C_3}{\mathrm{A}_i'} \sum_{j=1}^{N} \lambda_j \sum\nolimits_p \sum\nolimits_m \Theta_j^{-1}. \quad (25-c)$$

Substituting (25) into (24), we can obtain

$$SOP\left(C_{th}\right) = \frac{N_T}{\bar{\gamma}_A} \sum_{i=0}^{N_T-1} \left(\begin{array}{c} N_T-1 \\ i \end{array} \right) \frac{(-1)^i}{\mathrm{A}_i'} \sum_{j=1}^{N} \lambda_j \sum\nolimits_p \cdot \sum\nolimits_m \left(2C_1\Theta_j^{-3} + C_2\Theta_j^{-2} + C_3\Theta_j^{-1}\right). \quad (26)$$

As suggested by [52], in the high SNR regime with $\bar{\gamma}_A \to \infty$, the asymptotic SOP can be expressed as

$$SOP_{\bar{\gamma}_A \to \infty} = \left(\Psi \bar{\gamma}_A\right)^{-\Phi} + o\left(\bar{\gamma}_A^{-\Phi}\right), \quad (27)$$

where $o(\cdot)$ denotes higher order terms, $\Phi = 1$ is the secrecy diversity gain[3], and Ψ determines the slope of the asymptotic outage probability curve, which can be expressed as

$$\Psi = \left[N_T \sum_{i=0}^{N_T-1} \left(\begin{array}{c} N_T-1 \\ i \end{array} \right) \frac{(-1)^i}{\mathrm{A}_i'} \sum_{j=1}^{N} \lambda_j \sum\nolimits_p \cdot \sum\nolimits_m \left(\frac{\alpha}{\Theta_j^2} + \frac{\alpha-1}{\Theta_j} \right) \right]^{-1}. \quad (28)$$

[3]As shown in Eq. (26), the number of the power of $\bar{\gamma}_A$ is -1. Then, according to [52], when $\bar{\gamma}_A \to \infty$, it is easy to obtain $\Phi = 1$ by substituting the limitations of C_1, C_2 and C_3, ${C_1}^{\infty} = 0$, ${C_2}^{\infty} = \alpha$ and ${C_3}^{\infty} = \alpha - 1$, into Eq. (26).

IV. Secrecy capacity analysis

In this section, we will derive the analytical expression for the ASC.

The ASC can be given by

$$\bar{C}_s\left(\gamma_g, \gamma_{\max}\right) = E\left[C_s\left(\gamma_g, \gamma_{\max}\right)\right] = \int_0^{\infty} \int_0^{\infty} C_s\left(\gamma_g, \gamma_{\max}\right) f\left(\gamma_g, \gamma_{\max}\right) d\gamma_g d\gamma_{\max}, \quad (29)$$

where $f\left(\gamma_g, \gamma_{\max}\right)$ is the joint PDF of γ_g and $\gamma_{\max}$.

As all channels experience independent fading, we can further have the ASC as

$$\bar{C}_s\left(\gamma_{\mathrm{IR}}, \gamma_{\max}\right) = \frac{1}{\ln 2}\left(\bar{C}_{s1} - \bar{C}_{s2}\right), \quad (30)$$

where

$$\bar{C}_{s1} = \int_0^{\infty} \ln(1+x) f_{\gamma_g}(x) \int_0^{x} f_{\gamma_{\max}}(y)\, dy dx$$

and

$$\bar{C}_{s2} = \int_0^{\infty} \ln(1+y) f_{\gamma_{\max}}(y) \int_y^{\infty} f_{\gamma_g}(x)\, dx dy.$$

Using (19), we can rewrite $\bar{C}_{s1}$ as

$$\bar{C}_{s1} = \int_0^{\infty} \ln(1+x) f_{\gamma_g}(x) \sum_{i=1}^{N} \lambda_i \sum\nolimits_p \sum\nolimits_m \int_0^{x} \exp\left(-\Theta_i y\right) dy dx$$

$$= \sum_{i=1}^{N} \lambda_i \sum\nolimits_p \sum\nolimits_m \frac{1}{\Theta_i} \cdot \int_0^{\infty} \ln(1+x)\left(1 - \exp\left(-\Theta_i x\right)\right) f_{\gamma_g}(x) dx. \quad (31)$$

The integral in (31) can be written as

$$\int_0^{\infty} \ln(1+x)\left(1 - \exp\left(-\Theta_i x\right)\right) f_{\gamma_g}(x) dx = \int_0^{\infty} \ln(1+x) f_{\gamma_g}(x) dx - \int_0^{\infty} \ln(1+x) \exp\left(-\Theta_i x\right) f_{\gamma_g}(x) dx = I_A - I_B, \quad (32)$$

where $I_A = \int_0^{\infty} \ln(1+x) f_{\gamma_g}(x) dx$ and $I_B = \int_0^{\infty} \ln(1+x) \exp\left(-\Theta_i x\right) f_{\gamma_g}(x) dx$.

Using (15) and Eq. (2.6.23.5) in [51], we can obtain

$$I_A = N_T \sum_{j=0}^{N_T-1} \left(\begin{array}{c} N_T-1 \\ j \end{array} \right) (-1)^j A_j \cdot \int_0^{\infty} \ln(1+x) \exp\left(-B_j x\right) dx$$

$$= -N_T \sum_{j=0}^{N_T-1} \binom{N_T-1}{j} \frac{(-1)^j A_j}{B_j} \exp(B_j) \operatorname{Ei}(-B_j) \tag{33}$$

$$I_B = N_T \sum_{j=0}^{N_T-1} \binom{N_T-1}{j} (-1)^j A_j \cdot \int_0^{\infty} \ln(1+x) \exp(-(\Theta_i + B_j)x) dx$$

$$= -N_T \sum_{j=0}^{N_T-1} \binom{N_T-1}{j} \frac{(-1)^j A_j}{\Theta_i + B_j} \cdot \exp(\Theta_i + B_j) \operatorname{Ei}(-(\Theta_i + B_j)), \tag{34}$$

where $\operatorname{Ei}(x) = -\int_{-x}^{\infty} \frac{\exp(-t)}{t} dt$ is the exponential integral function.

Then, $\bar{C}_{s1}$ can be obtained by substituting (32), (33) and (34) into (31).

Using (15) and (19), we can rewrite $\bar{C}_{s2}$ as

$$\bar{C}_{s2} = N_T \sum_{i=0}^{N_T-1} \binom{N_T-1}{i} (-1)^i A_i \int_0^{\infty} \ln(1+y) \cdot f_{\gamma_{\max}}(y) \int_y^{\infty} \exp(-B_i x) dx dy$$

$$= N_T \sum_{i=0}^{N_T-1} \binom{N_T-1}{i} \frac{(-1)^i A_i}{B_i} \int_0^{\infty} \ln(1+y) \cdot \exp(-B_i y) f_{\gamma_{\max}}(y) dy$$

$$= N_T \sum_{i=0}^{N_T-1} \binom{N_T-1}{i} \frac{(-1)^i A_i}{B_i} \sum_{j=1}^{N} \lambda_j \sum_p \sum_m \cdot \int_0^{\infty} \ln(1+y) \exp(-(\Psi + B_i)y) dy, \tag{35}$$

where $\Psi = \boldsymbol{\lambda}_{p,m}^T \mathbf{I}_p + \lambda_j$.

Using Eq. (2.6.23.5) in [51], we can rewrite the integral in last equation as

$$\int_0^{\infty} \ln(1+y) \exp(-(\Psi + B_i)y) dy = -\frac{\exp((\Psi + B_i)y)}{(\Psi + B_i)} \cdot \operatorname{Ei}(-(\Psi + B_i)). \tag{36}$$

So, $\bar{C}_{s2}$ can be obtained by substituting (36) into (35).

Therefore, the ASC can be calculated by substituting $\bar{C}_{s1}$ and $\bar{C}_{s2}$ into (30).

V. The tradeoff between Energy Harvesting and Information Eavesdropping

In this section, we focus on the optimization problem to achieve the tradeoff between EH and information eavesdropping at ERs. It is worth noting that the total power of the received signal at each ER is limited. Then, the PS factor, ρ_i ($i \in \{1, \cdots, N\}$), plays an important role on the performance of ERs, because if more power of the received signal is split to the ID, higher SNR at each ER can be obtained, as shown by (5-b), which will lead to higher eavesdropping capacity in the end. However, there will be less signal power left for EH in return, which should lead to the decrease in the available transmit power for ERs to deliver the eavesdropped information. Therefore, in this section we propose a method how to find out the optimal PS factor at each ER to achieve the tradeoff between the EH and the information eavesdropping.

To formulate the optimization problem, we assume that all ERs will use the harvested energy to transmit the eavesdropped information to the same sink and denote the channel gain between the ith ER and the sink as w_i, which experiences independent but not necessarily identical Rayleigh fading.

It is easy to obtain the eavesdropping capacity and the harvested energy at the ith ER as

$$C_{\mathrm{BS}i} = \log_2(1 + \gamma_{\mathrm{EH}i}) = \log_2\left(1 + \frac{\rho_i P_t L_c |h_i|^2}{{d_{\mathrm{B,E}_i}}^{\kappa} (\rho_i N_0 + \sigma_i^2)}\right) \tag{37-a}$$

and

$$E_i = \frac{(1-\rho_i) P_t L_c |h_i|^2 T_1}{{d_{\mathrm{B,E}_i}}^{\kappa}}, \tag{37-b}$$

respectively, where T_1 is the time for the information delivery between BS and IR.

Then, the received signal at the sink from the ith ER can be written as

$$y_{\mathrm{sink}i} = \sqrt{(E_i + E_{\mathrm{bud}i}) L_c {d_{\mathrm{E}i,\mathrm{S}}}^{-\kappa} / T_2} w_i s_i' + n_{\mathrm{sink}}, \tag{38}$$

where $d_{\mathrm{E}i,\mathrm{S}}$ is the distance between the ith ER and the sink, T_2 is the time spent on the information transmission between the sink and the ith ER, s_i' is the eavesdropped information bits transmitted from the ith ER to the sink, $E_{\mathrm{bud}i} \geq 0$ is the portion of the transmit energy, which comes from the local budget at the ith ER and not from the EH process, n_{sink} is the complex Gaussian noise at the sink with zero means and unit variance. For simplification, we also assume the links between ERs and the sink are with the same path loss constant as the links between BS and ERs.

Therefore, the SNR of the link between the sink and the ith ER can be achieved as $\gamma_{\mathrm{sink}i} = \frac{(1-\rho_i) P_t L_c^2 |h_i|^2 |w_i|^2 T_1}{{d_{\mathrm{B,E}_i}}^{\kappa} {d_{\mathrm{E}i,\mathrm{S}}}^{\kappa} T_2} + \frac{E_{\mathrm{bud}i} L_c |w_i|^2}{{d_{\mathrm{E}i,\mathrm{S}}}^{\kappa} T_2}$. So the channel capacity of the link from the ith ER to the sink can be easily presented as

$$C_{\mathrm{sink}i} = \log_2(1 + \gamma_{\mathrm{sink}i}) = \log_2\left(1 + \frac{(1-\rho_i) P_t L_c^2 |h_i|^2 |w_i|^2 T_1}{{d_{\mathrm{B,E}_i}}^{\kappa} {d_{\mathrm{E}i,\mathrm{S}}}^{\kappa} T_2} + \frac{E_{\mathrm{bud}i} L_c |w_i|^2}{{d_{\mathrm{E}i,\mathrm{S}}}^{\kappa} T_2}\right). \tag{39}$$

Then, to promise all the eavesdropped information bits at the ith ER can be transmitted to the sink, the eavesdropping throughput of the eavesdropping link between BS and the ith ER should not be larger than the throughput of the link between the sink and of the ith ER. So the criterion, $\Delta = T_1 C_{\mathrm{BS}i} - T_2 C_{\mathrm{sink}i} \leq 0$, should be satisfied, namely, it holds

$$\Delta = T_1 \log_2\left(1 + \frac{\rho_i P_t L_c |h_i|^2}{{d_{\mathrm{B,E}_i}}^{\kappa}(\rho_i N_0 + \sigma_i^2)}\right) - T_2 \log_2\left(1 + \frac{(1-\rho_i) P_t L_c^2 |h_i|^2 |w_i|^2 T_1}{{d_{\mathrm{B,E}_i}}^{\kappa} {d_{\mathrm{E}i,\mathrm{S}}}^{\kappa} T_2} + \frac{E_{\mathrm{bud}i} L_c |w_i|^2}{{d_{\mathrm{E}i,\mathrm{S}}}^{\kappa} T_2}\right) \leq 0. \tag{40}$$

Finally, the optimal PS factor for the ith ER can be numerically searched and calculated within the interval $[0, 1]$ to realize the optimal balance EH and information eavesdropping.

Specially, we can obtain the optimal PS factor in the case of $T_1/T_2 = 1$ as

$$\rho_{opt} = \frac{\sqrt{(a + bd - cN_0)^2 + 4b(b+c)N_0\sigma_i^2} - a - bd + cN_0}{2bN_0}. \tag{41}$$

where $a = \frac{P_t L_c |h_i|^2}{{d_{\mathrm{B,E}_i}}^{\kappa}}$, $b = \frac{P_t L_c^2 |h_i|^2 |w_i|^2}{{d_{\mathrm{B,E}_i}}^{\kappa} {d_{\mathrm{E}i,\mathrm{S}}}^{\kappa}}$, $c = \frac{E_{\mathrm{bud}i} L_c |w_i|^2}{{d_{\mathrm{E}i,\mathrm{S}}}^{\kappa} T_2}$ and $d = \sigma_i^2 - N_0$.

VI. Numerical results and discussion

In this section, we compare simulation and analysis results for SOP and ASC, and present the effect of the system settings on choosing the optimal PS factor. Unless otherwise explicitly specified, the parameters are set as P_t = 30 dBm, $d_{\mathrm{B,I}}$ = 10 m, $d_{\mathrm{B,E}_i}$ = 2 m, $\eta = 0$, g_A = 1, $N_T = N = 2$, N_0 = 1, σ_i^2 = 1 ($i \in \{1, \cdots, N\}$), $\rho_i = \rho$ = 0.5 ($i \in \{1, \cdots, N\}$), $L_c = 35.97 \times 10^{-4}$ (when the antenna gains of BS, IR and ER are 18 dBi, -2 dBi and -2 dBi, and the carrier frequency is 1000 MHz), and C_{th} = 0 dB. Simulation is performed by transmitting 1×10^6 bits and $\tau = g_A/\bar{h}$, where $\bar{h}$ is the average value of h_{Ai} ($i \in \{1, \cdots, N\}$) and $h_{Aj+1} = h_{Aj} + 0.2$ ($j \in \{1, \cdots, N-1\}$).

A. The effect of small-scale fading

In Figs. 1-3, we present simulation and analytical results of SOP v.s. τ for various combinations of ρ and η, P_t/N_0 and combinations of N and N_T, respectively. Clearly, analytical results perfectly match with Monte-Carlo simulations, and SOP can be improved while τ increases, because a higher τ represents that the channel condition for BS-IR link outperforms the ones of BS-ER eavesdropping links.

As depicted in Fig. 1, the SOP with a lower ρ outperforms the one with a higher ρ. Because a higher ρ means a larger portion of the received signal power is split to the ID at each ER, then a higher received SNR at the ID of each ER, resulting in a higher eavesdropping capacity. Meanwhile, we can also see that the SOP with a higher η outperforms the one with a lower η due to the factor that a higher η represents a higher correlation between the channel gain of the link between the

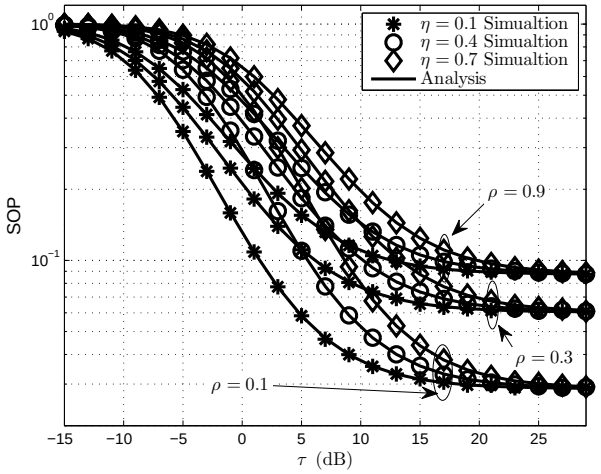

Fig. 1. SOP vs. τ for various combinations of ρ and η

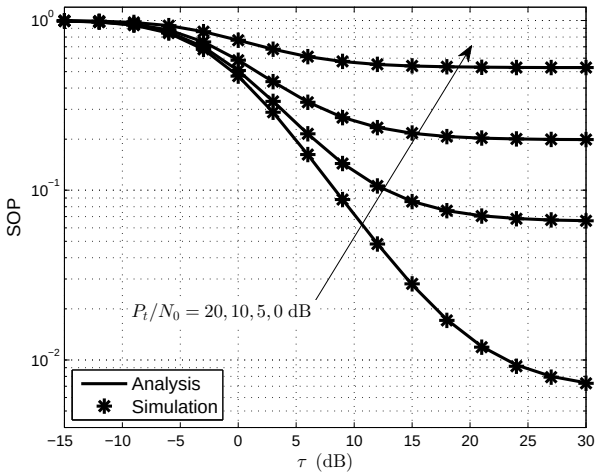

Fig. 2. SOP vs. τ for various P_t/N_0

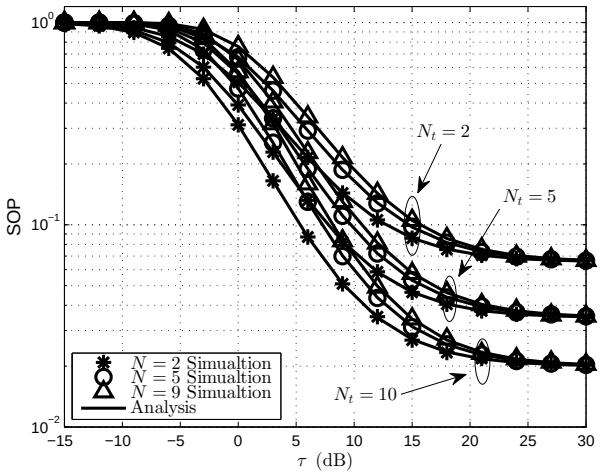

Fig. 3. SOP vs. τ for various combinations of N and N_T

selected transmit antenna at BS and IR, g, and the one of the link between the selected transmit antenna at BS and IR at the selection instant, $\tilde{g}$, which can be demonstrated by Eq. (3) in Section II.

In Fig. 2, we can observe that SOP can be improved by increasing P_t/N_0. The received SNR at IR can be improved more greatly than the one at each ER through increasing the transmit power at the BS because of the diversity gain achieved by the TAS scheme adopted at the BS.

As shown in Fig. 3, the SOP with a larger N_T outperforms the one with a smaller N_T due to the larger diversity gain benefited from the TAS scheme adopted at the BS. Further, the SOP with a small N outperforms the one with a large N. It is because of a lower virtual diversity gain achieved among the ERs for the case of a smaller N. This can be easily explained by the definition of $\gamma_{\max}$ as shown below Eq. (6) in Section II.

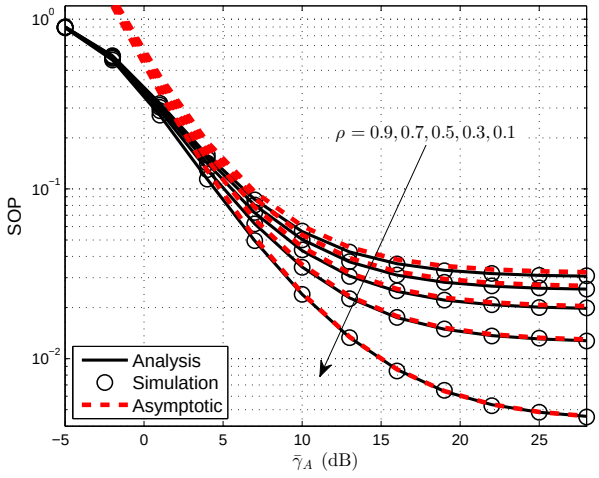

Fig. 4. SOP vs. $\bar{\gamma}_A$ for various ρ

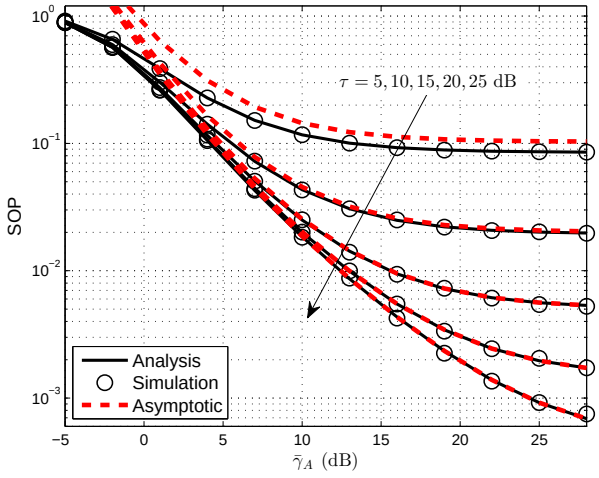

Fig. 5. SOP vs. $\bar{\gamma}_A$ for various τ

Figs. 4 and 5 present the SOP vs. $\bar{\gamma}_A$ for various ρ and τ, respectively, while $N_T = 3$ and $N = 4$, and the link channels between BS and each ER experience independent and identically distributed Rayleigh fading. The asymptotic results for SOP are obtained from (27) in Section III. We can observe that our asymptotic results accurately predict the secrecy diversity order and secrecy diversity gain. As shown in Fig. 4, it can also be seen that the SOP with a lower ρ outperforms the one with a higher ρ. It is because that a lower ρ means less received signal power consumed on information decoding, leading to a better SOP performance. Furthermore, it is clear that in Fig. 5 the SOP with a higher τ outperforms the one with a lower τ. Because the BS-IR link gets better compared to BS-ER links as τ increases.

In Figs. 6-8, we present simulation and analytical results of ASC vs. τ for various combinations of ρ and η, P_t/N_0 and combinations of N and N_T, respectively. It is clear that simulation and analytical results perfectly match with each other. Similar to the observations from Figs. 1-3, ASC can be improved while τ increasing, as a higher τ represents the case that the channel condition for BS-IR link outperforms the one of BS-ER eavesdropping links.

As shown in Fig. 6, the ASC with a lower ρ outperforms the one with a higher ρ. This is because that a lower ρ means less signal power is distributed to the ID and more power is split to the energy harvester at each ER, leading to a lower received SNR at each ER, in turn, a lower eavesdropping capacity. Further, one can observe that the ASC with a higher η outperforms the one with a lower η. This can be easily explained by the same reason as presented for the observation of Fig. 1.

As shown in Fig. 7, ASC can be improved while increasing P_t/N_0. The received SNR at IR can be improved more greatly than the one at each ER when the transmit power increases at the BS because of the diversity gain obtained by the adopted TAS scheme adopted at IR.

In Fig. 8, due to a larger diversity gain obtained by the TAS scheme adopted at the BS, the ASC with a larger N_T outperforms the one with a smaller N_T. We can also see that the ASC with a small N outperforms the one with a larger N. The same reason for Fig. 3 can explain this finding: a lower virtual diversity gain can be obtained among the ERs for the case of a smaller N, which can be explained by the definition of $\gamma_{\max}$ as shown below Eq. (6) in Section II. Further, we can also find that N has a weaker effect on the ASC in high τ region for various N_T compared to the ones in lower τ region. A similar finding can be obtained for the effect N_T on ASC.

B. The effect of both small-scale fading and path-loss

As the received signal power always suffers from path-loss in cellular networks, in this subsection we will discuss the effect of path-loss on the secrecy performance of the target MISO system.

Figs. 9 and 10 depicts the SOP and ASC for various κ in presence of both small-scale fading and path-loss while P_t = 50 dBm, ρ = 0.1, N = 2, N_T = 4 and 8, and $C_{th} = -18$ dB, respectively. Obviously, the SOP and ASC with a lower κ outperforms the ones with a higher κ. Because a higher κ represents a strong path-loss suffered by the transmitted signals, resulting in a lower received signal power.

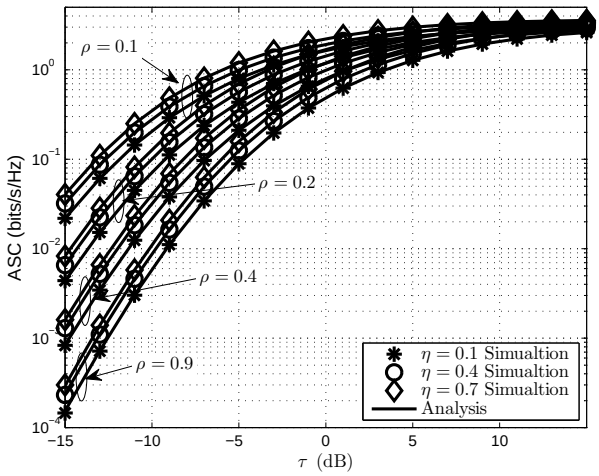

Fig. 6. ASC vs. τ for various combinations of ρ and η

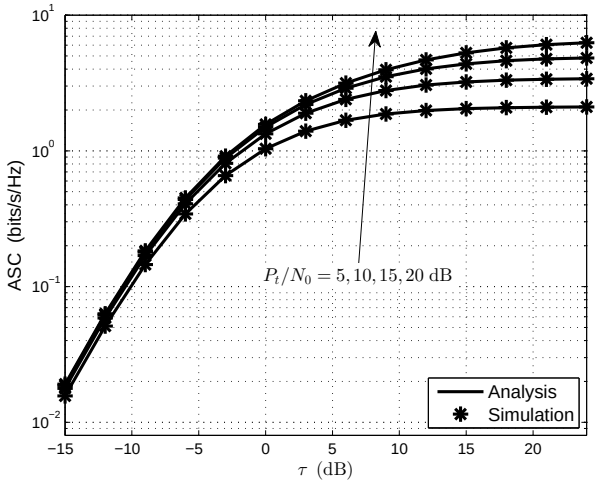

Fig. 7. ASC vs. τ for various P_t/N_0

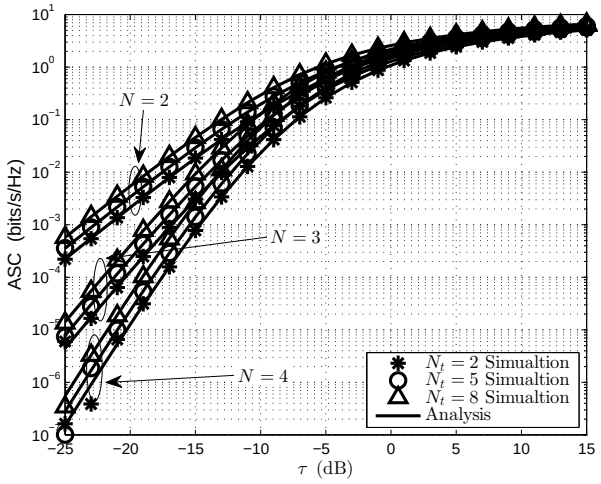

Fig. 8. ASC vs. τ for various combinations of N and N_T

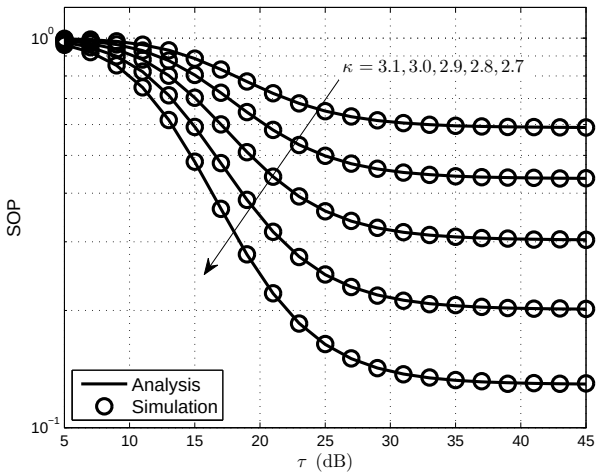

Fig. 9. SOP for various κ

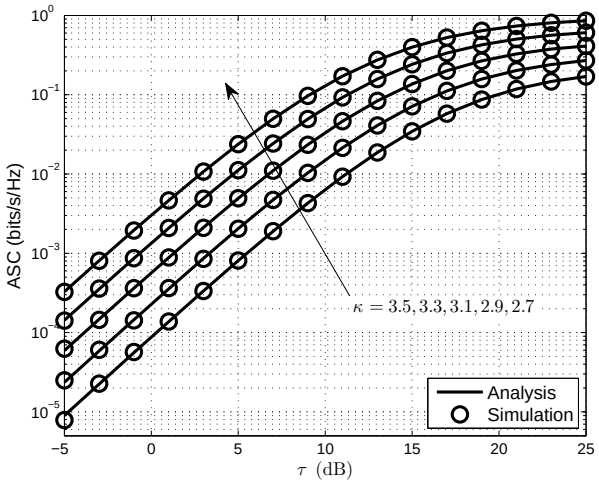

Fig. 10. ASC for various κ

We can also find that the ASC obtained in Fig. 12 is quite lower than the ones in Figs. 6-8, due to the effect of path-loss.

Moreover, we can easily see that in high κ region there exists a floor for SOP in Figs. 1-3 and 9, and a ceiling for ASC in Figs. 6-8 and 10. It can be easily explained by (5) in Section II. The instantaneous secrecy capacity has a limitation, $\log_2(1+\gamma_{\mathrm{IR}})$, because increasing κ means that BS-IR link outperforms BS-ER eavesdropping links.

C. The optimal power splitting factor

In this subsection, we focus on the effect of small-scale fading for simplification while the main parameters are set as $E_{\mathrm{budi}} = 0$, $T_1 = 1$. Fig. 11 demonstrates the relationship between $|\Delta|$ and ρ for various combinations of P_t/N_0 and T_1/T_2 from Eq. (40). The figure implies that there exists a unique optimal PS factor, which makes $|\Delta| = 0$ and can achieve the tradeoff between information eavesdropping and EH as suggested by Eq. (40). We also find that, when $T_1/T_2 = 2$, the optimal PS factor increases while P_t/N_0

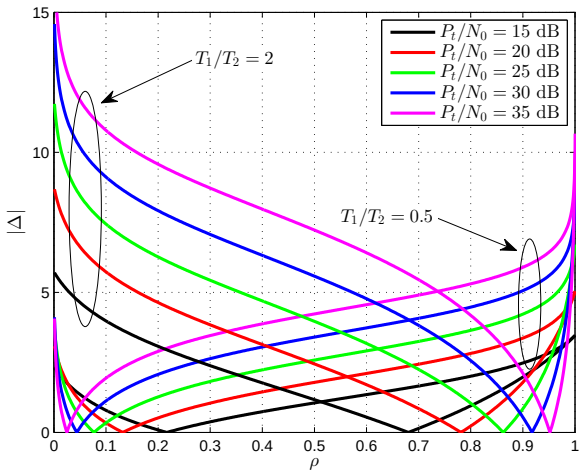

Fig. 11. The relationship of $|\Delta|$ and ρ for various P_t/N_0

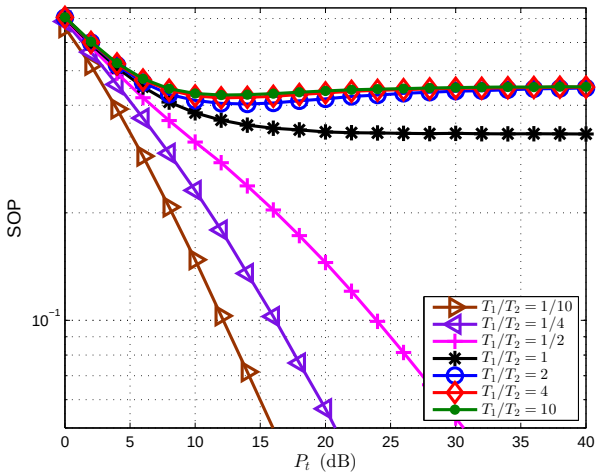

Fig. 12. The SOP for optimal ρ

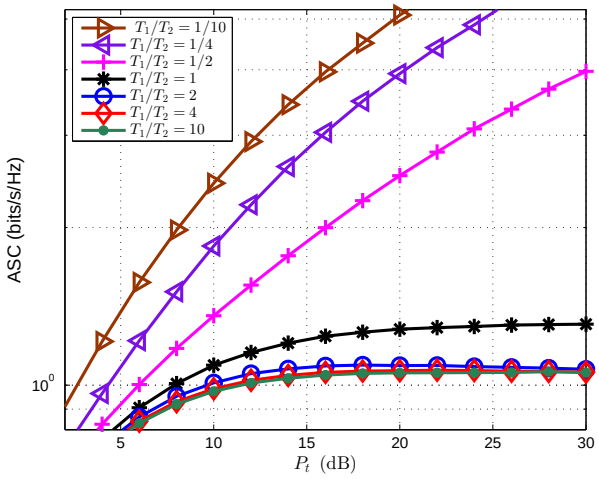

Fig. 13. The ASC for optimal ρ

increasing, it is because in this case more energy can be harvested to deliver the eavesdropped information with a same PS factor, then more power of the received signal can be used to for information decoding.

Moreover, as shown in Fig. 11 totally opposite observations can be obtained for $T_1/T_2 = 0.5$ compared with the ones for $T_1/T_2 = 2$. It can be explained by the fact that there are more time for energy harvesting for $T_1/T_2 = 2$ compared with $T_1/T_2 = 0.5$, then ER can choose a larger ρ to split more signal energy for information eavesdropping.

In Fig. 12, we present the SOP for optimal ρ with various T_1/T_2. It is obvious that the SOP for $T_1/T_2 \geq 1$ is improved while P_t/N_0 increasing, due to the decreased optimal ρ. One can also observe that the SOP for $T_1/T_2 = 1/2, 1/4$ and 1/10 is improved by increasing P_t/N_0 while $P_t/N_0 < 12$ dB. However, when $P_t/N_0 \geq 12$ dB, the SOP for $T_1/T_2 = 1/2, 1/4$ and 1/10 gets bad while P_t/N_0 increasing. It is because the optimal ρ will increases when P_t/N_0 increases, resulting in a higher eavesdropping capacity as suggested by Eq. (37-a), which causes a higher outage probability. In high P_t/N_0 region, the improving effect of the optimal ρ on the eavesdropping capacity outperforms the one of increasing P_t/N_0 on the capacity of BS-IR link.

Fig. 13 depicts the ASC for optimal ρ with various T_1/T_2. The ASC for $T_1/T_2 \geq 1$ increases while P_t/N_0 increasing, as the optimal ρ will decreases as P_t/N_0 increases. Further, it is seen that in low P_t/N_0 region (< 20 dB) the ASC for $T_1/T_2 = 1/2, 1/4$ and 1/10 increases when P_t/N_0 increases, and in high P_t/N_0 region (≥ 20 dB) the ASC for $T_1/T_2 = 1/2, 1/4$ and 1/10 decreases while P_t/N_0 increasing. The explanation on the observation in Fig. 12 can be readily used to interpret this finding.

VII. Conclusion

In this paper, we have investigated the secrecy performance of multiple-input single-output simultaneous wireless information and power transfer systems in the presence of imperfect CSI. By considering that the information delivery between the base station and information receiver may be overheard by malicious energy-harvesting receivers, secrecy outage and average secrecy capacity have been studied with imperfect CSI. The closed-form analytical expressions for the exact and the asymptotic secrecy outage probability, and the average secrecy capacity have been respectively derived while each eavesdropping link experiences independent not necessarily identically Rayleigh fading. The validity of the proposed analytical models has been verified through Monte-Carlo simulations. Moreover, the optimal PS factor is studied for each ER to realize the tradeoff between the energy harvesting and the information eavesdropping. Our results can reveal the impact of the imperfect CSI on the secrecy performance of the target systems and the analysis performed in this paper will be beneficial for the design and optimization of practical MISO SWIPT system as imperfect CSI (including time delay and Doppler frequency shift) is considered during the derivation.

REFERENCES

[1] L. R. Varshney, "Transporting information and energy simultaneously," in *Proc. IEEE Int. Symp. Inf. Theory (ISIT)*, Toronto, Canada, Jul. 2008, pp. 1612-1616.

[2] P. Grover and A. Sahai, "Shannon meets Tesla: Wireless information and power transfer," in *Proc. 2010 IEEE Int. Symp. Inf. Theory*, Austin, TX, USA, June 13-18, 2010, pp. 2363-2367.

[3] M. Zhang, and Y. Liu, "Energy harvesting for physical-layer security in OFDMA networks," *IEEE Trans. Inf. Forensics Security*, vol. 11, no. 1, pp. 154-162, Jan. 2016.

[4] J. Xu, L. Liu, and R. Zhang, "Multiuser MISO beamforming for simultaneous wireless information and power transfer," *IEEE Trans. Sig. Proc.*, vol. 62, no. 18, pp. 4798-4810, Sept. 2014.

[5] Q. Li, Q. Zhang, and J. Qin, "Secure Relay beamforming for simultaneous wireless information and power transfer in nonregenerative relay networks," *IEEE Trans. Veh. Tech.*, vol. 63, no. 5, pp. 2462-2467, May 2014.

[6] Q. Shi, L. Liu, W. Xu, and R. Zhang, "Joint transmit beamforming and receive power splitting for MISO SWIPT systems," *IEEE Trans. Wireless Commun.*, vol. 13, no. 6, pp. 3269-3280, June 2014.

[7] Y. Zeng and R. Zhang, "Full-duplex wireless-powered relay with self-energy recycling," *IEEE Wireless Commun. Lett.*, vol. 4, no. 2, pp. 201-204, Apr. 2015.

[8] B. Zhu, J. Ge, Y. Huang, Y. Yang, and M. Lin, "Rank-two beamformed secure multicasting for wireless information and power transfer," *IEEE Sig. Proc. Lett.*, vol. 22, no. 6, pp.723-727, June 2015.

[9] L. Liu, R. Zhang, and K. C. Chua, "Secrecy wireless information and power transfer with MISO beamforming," *IEEE Trans. Sig. Proc.*, vol. 62, no. 7, pp. 1850-1863, April 2014.

[10] H. Zhang, C. Li, Y. Huang, and L. Yang, "Secure beamforming for SWIPT in multiuser MISO broadcast channel with confidential messages," *IEEE Commun. Lett.*, vol. 19, no. 8, pp. 1347-1350, Aug. 2015.

[11] X. Zhao, J. Xiao, Q. Li, Q. Zhang, and J. Qin, "Joint optimization of AN-aided transmission and power splitting for MISO secure communications with SWIPT," *IEEE Commun. Lett.*, vol. 19, no. 11, pp. 1969-1972, Nov. 2015.

[12] R. Zhang and C. K. Ho, "MIMO broadcasting for simultaneous wireless information and power transfer," *IEEE Trans. Wireless Commun.*, vol. 12, no. 5, pp. 1989-2001, May 2013.

[13] X. Zhou, R. Zhang, and C. K. Ho, "Wireless information and power transfer in multiuser OFDM systems," *IEEE Trans. Wireless Commun.*, vol. 13, no. 4, pp. 2282-2294, April 2014.

[14] J. Park and B. Clerckx, "Joint wireless information and energy transfer in a two-user MIMO interference channel," *IEEE Trans. Wireless Commun.*, vol 12, no 8, pp. 4210-4221, Aug 2013.

[15] R. Zhang, L.-L. Yang and L. Hanzo, "Energy pattern aided simultaneous wireless information and power transfer, *IEEE J. Sel. Areas in Commun.*, vol. 33, no. 8, pp. 1492-1504, Aug. 2015.

[16] H. Xing, L. Liu, and R. Zhang, "Secrecy wireless information and power transfer in fading wiretap channel," to appear in *IEEE Trans. Veh. Tech.*, DOI: 10.1109/TVT.2015.2395725.

[17] Q. Shi, W. Xu, J. Wu, E. Song, and Y. Wang, "Secure beamforming for MIMO broadcasting with wireless information and power transfer," *IEEE Trans. Wireless Commun.*, vol 14, no 5, pp. 2841-2853, May 2015.

[18] B. Fang, Z. Qian, W. Zhong, and W. Shao, "AN-aided secrecy precoding for SWIPT in cognitive MIMO broadcast channels," *IEEE Commun. Lett.*, vol. 19, no. 9, pp. 1632-1635, Sept. 2015.

[19] W. Wu and B.aoyun Wang, "Efficient transmission solutions for MIMO wiretap channels with SWIPT," *IEEE Commun. Lett.*, vol. 19, no. 9, pp. 1548-1551, Sept. 2015.

[20] M. J. Gans, "The effect of Gaussian error in maximal ratio combiners," *IEEE Trans. Commun. Technol.*, vol. 19, pp. 492-500, Aug. 1971.

[21] A. P. Liavas, "Tomlinson-Harashima precoding with partial channel knowledge," *IEEE Trans. Commun.*, vol. 53, no. 1, pp. 5-9, Jan. 2005.

[22] Derrick W. K. Ng, Ernest S. Lo, and R. Schober, "Robust beamforming for secure communication in systems with wireless information and power transfer," *IEEE Trans. Wireless Commun.*, vol. 13, no. 8, pp. 4599-4615, Aug. 2014.

[23] Q. Zhang, X. Huang, Q. Li, and J. Qin, "Cooperative jamming aided robust secure transmission for wireless information and power transfer in MISO channels," *IEEE Trans. Commun.*, vol. 63, no. 3, pp. 906-915, Mar. 2015.

[24] Q. Shi, W. Xu, T.-H. Chang, Y. Wang, and E. Song, "Joint beamforming and power splitting for MISO interference channel with SWIPT: An SOCP relaxation and decentralized algorithm," *IEEE Trans. Sig. Proc.*, vol. 62, no. 12, pp. 6194-6208, Dec. 2014.

[25] M. R. A. Khandaker and K.-K. Wong, "SWIPT in MISO multicasting systems," *IEEE Wireless Commun. Lett.*, vol. 3, no. 3, pp. 277-280, June 2014.

[26] F. Wang, T. Peng, Y. Huang and X. Wang, "Robust transceiver optimization for power-splitting based downlink MISO SWIPT systems," *IEEE Sig. Proc. Lett.*, vol. 22, no. 9, pp. 1492-1496, Sept. 2015.

[27] R. Feng, Q. Li, Q. Zhang, J. Qin, "Robust secure transmission in MISO simultaneous wireless information and power transfer system," *IEEE Trans. Veh. Tech.*, vol. 64, no. 1, pp. 400-405, Jan. 2015.

[28] M. Tian, X. Huang, Q. Zhang, Jiayin Qin, "Robust AN-aided secure transmission scheme in MISO channels with simultaneous wireless information and power transfer," *IEEE Sig. Proc. Lett.*, vol. 22, no. 6, pp.723-727, June 2015.

[29] Derrick W. K. Ng, Ernest S. Lo, and R. Schober, "Multi-objective resource allocation for secure communication in cognitive radio networks with wireless information and power transfer," to appear in *IEEE Trans. Veh. Tech.*, DOI: 10.1109/TVT.2015.2395725.

[30] C. Xing, N. Wang, J. Ni, Z. Fei, and J. Kuang, "MIMO beamforming designs with partial CSI under energy harvesting constraints," *IEEE Sig. Proc. Lett.*, vol. 20, no. 4, pp. 363-366, Apr. 2013.

[31] Q. Sun, L. Li, and J. Mao, "Simultaneous information and power transfer scheme for energy efficient MIMO systems," *IEEE Commun. Lett.*, vol. 18, no. 4, pp. 600-603, Apr. 2013.

[32] Z. Xiang and M. Tao, "Robust beamforming for wireless information and power transmission," *IEEE Wireless Commun. Lett.*, vol. 1, no. 4, pp. 372-375, Aug. 2012.

[33] C.-F. Liu, M. Maso, S. Lakshminarayana, C.-H. Lee, and Tony Q. S. Quek, "Simultaneous wireless information and power transfer under different CSI acquisition schemes," *IEEE Trans. Wireless Commun.*, vol. 14, no. 4, pp. 1911-1916, Apr. 2015.

[34] M. R. A. Khandaker and K.-K. Wong, "Robust secrecy beamforming with energy-harvesting eavesdroppers," *IEEE Wireless Commun. Lett.*, vol. 4, no. 1, pp. 10-13, Feb. 2015.

[35] J. Zhang, C. Yuen, C.-K. Wen, S. Jin, K.-K. Wong, and H. Zhu, "Large system secrecy rate analysis for SWIPT MIMO wiretap channels," *IEEE Trans. Inf. Forensics Security*, vol. 11, no. 1, pp. 74-85, Jan. 2016.

[36] R. Liu and W. Trappe, *Securing wireless communications at the physical layer*. New York: Springer, 2009.

[37] M. R. Bloch and J. N. Laneman, "Exploiting partial channel state information for secrecy over wireless channels," *IEEE J. Sel. Areas in Commun.*, vol. 31, no. 9, pp. 1840-1849, Sept. 2013.

[38] J. Li and A. P. Petropulu, "Explicit solution of worst-case secrecy rate for MISO wiretap channels with spherical uncertainty," *IEEE Trans. Sig. Proc.*, vol. 60, no. 7, pp. 3892-3895, Dec. 2012.

[39] A. Mukherjee and A. L. Swindlehurst, "Robust beamforming for security in MIMO wiretap channels with imperfect CSI," *IEEE Trans. Sig. Proc.*, vol. 59, no. 1, pp. 351-361, Dec. 2011.

[40] Z. Rezki, A. Khisti, M.-S. Alouini, "On the secrecy capacity of the wiretap channel with imperfect main channel estimation," *IEEE Trans. Commun.*, vol. 62, no. 10, pp. 3652-3664, Oct. 2014.

[41] S.-C. Lin, T.-H. Chang, Y.-L. Liang, Y. Hong, and C.-Y. Chi, "On the impact of quantized channel feedback in guaranteeing secrecy with artificial noise: The noise leakage problem," *IEEE Trans. Wireless Commun.*, vol. 10, no. 3, pp. 901-915, Mar. 2011.

[42] S. Gerbracht, C. Scheunert, and E. Jorswieck, "Secrecy outage in MISO systems with partial channel information," *IEEE Trans. Inf. Forensics Security*, vol. 7, no. 2, pp. 704-716, Apr. 2012.

[43] S. Ma, M. Hong, E. Song, X. Wang, and D. Sun, "Outage constrained robust secure transmission for MISO wiretap channels," *IEEE Trans. Wireless Commun.*, vol. 13, no. 10, pp. 5558-5570, Oct. 2014.

[44] Muhammad R. A. Khandaker, and Kai-Kit Wong, "Masked beamforming in the presence of energy-harvesting eavesdroppers," *IEEE Trans. Inf. Forensics and Security*, vol. 10, no. 1, pp. 40-54, Jan. 2015.

[45] G. Pan, C. Tang, T. Li, and Y. Chen. "Secrecy performance analysis for SIMO simultaneous wireless information and power transfer systems," *IEEE Trans. Commun.*, vol. 63, no. 9, pp. 3423-3433, Sept. 2015.

[46] S. Prakash and I. McLoughlin, "Effects of Channel Prediction for Transmit Antenna Selection With Maximal-Ratio Combining in Rayleigh Fading," *IEEE Trans. Veh. Tech.*, vol. 60, no. 6, pp. 2555-2568, July 2011.

[47] H. Lehpamer, *Transmission systems design handbook for wireless networks*, Boston: Artech House, 2002.

[48] I.S. Gradshteyn and I.M. Ryzhik, *Table of integrals, series and products, 7 Ed*. San Diego: Academic Press, 2007.

[49] J. López-Vicario, C. Antón-Haro, "Analytical assessment of multi-user vs. spatial diversity trade-offs with delayed channel state information," *IEEE Commun. Lett.*, vol. 10, no. 8, pp. 588-590, Aug. 2006.

[50] A. P. Prudnikov, Yu. A. Brychkov, and O. I. Marichev, *Integrals and series, vol. 2, special functions*. New York: Gordon & Breach Sci. Publ., 1986.

[51] A. P. Prudnikov, Yu. A. Brychkov, and O. I. Marichev, *Integrals and series, vol. 1, elementary functions*. New York: Gordon & Breach Sci. Publ., 1986.

[52] N. Yang, P. L. Yeoh, M. Elkashlan, R. Schober, and I. B. Collings, "Transmit antenna selection for security enhancement in MIMO wiretap channels," *IEEE Trans. Commun.*, vol. 61, no. 1, pp. 144-154, Jan. 2013.